AFRL-SN-RS-TR-1998-199
In-House Report
December 1998


# PHOTONICALLY GENERATED TRUE TIME DELAY FOR PHASED ARRAY APPLICATIONS

**Paul M. Payson, Henry Zmuda, Edward N. Toughlian, Richard A. Soref, Herbert W. Klumpe III, and Steven T. Johns**

*APPROVED FOR PUBLIC RELEASE; DISTRIBUTION UNLIMITED.*



**AIR FORCE RESEARCH LABORATORY
SENSORS DIRECTORATE
ROME RESEARCH SITE
ROME, NEW YORK**

This report has been reviewed by the Air Force Research Laboratory, Information Directorate, Public Affairs Office (IFOIPA) and is releasable to the National Technical Information Service (NTIS). At NTIS it will be releasable to the general public, including foreign nations.

AFRL-SN-RS-TR-1998-199 has been reviewed and is approved for publication.

APPROVED:

GREGORY J. ZAGAR
Chief, RF Photonics Branch
Sensors Directorate

FOR THE DIRECTOR:

ROBERT G. POLCE
Acting Chief, Rome Operations Office
Sensors Directorate

If your address has changed or if you wish to be removed from the Air Force Research Laboratory Rome Research Site mailing list, or if the addressee is no longer employed by your organization, please notify AFRL/SNDR, 25 Electronic Pky, Rome, NY 13441-4515. This will assist us in maintaining a current mailing list.

Do not return copies of this report unless contractual obligations or notices on a specific document require that it be returned.

| REPORT DOCUMENTATION PAGE | | | Form Approved OMB No. 0704-0188 |
|---|---|---|---|



| 1. AGENCY USE ONLY *(Leave blank)* | 2. REPORT DATE | 3. REPORT TYPE AND DATES COVERED |
|---|---|---|
| | December 1998 | In-House, Oct 96 - Sep 98 |

**4. TITLE AND SUBTITLE**

PHOTONICALLY GENERATED TRUE TIME DELAY FOR PHASED ARRAY APPLICATIONS

**5. FUNDING NUMBERS**

PE - 62702F
PR - 4600
TA - P1
WU- 37

**6. AUTHOR(S)**

Paul M. Payson, Richard A. Soref, Herbert W. Klumpe III, Steven T. Johns, AFRL; Henry Zmuda, Univ. of Florida; and Edward N. Toughlian, ENSCO Inc.

**7. PERFORMING ORGANIZATION NAME(S) AND ADDRESS(ES)**

Air Force Research Laboratory/SNDR
25 Electronic Pky
Rome, NY 13441-4515

**8. PERFORMING ORGANIZATION REPORT NUMBER**

AFRL-SN-RS-TR-1998-199

**9. SPONSORING/MONITORING AGENCY NAME(S) AND ADDRESS(ES)**

Air Force Research Laboratory/SNDR
25 Electronic Pky
Rome, NY 13441-4515

**10. SPONSORING/MONITORING AGENCY REPORT NUMBER**

AFRL-SN-RS-TR-1998-199

**11. SUPPLEMENTARY NOTES**

AFRL Project Engineer: Paul M. Payson/SNDR/(315) 330-7911

**12a. DISTRIBUTION AVAILABILITY STATEMENT**

APPROVED FOR PUBLIC RELEASE; DISTRIBUTION UNLIMITED.

**12b. DISTRIBUTION CODE**

**13. ABSTRACT** *(Maximum 200 words)*

Several relatively new photonic components have recently come to the forefront in applications related to the photonic processing of broadband microwave signals. Included in this set of photonic elements are the wavelength tunable laser, high dispersion optical fiber, and the Bragg reflection grating. These components hold the promise of revolutionizing the field of broadband photonic processing. This report documents the performance characteristics of these components and shows how they can be used for two broadband phased array applications, beamforming and null steering. Two systems are described. A technical overview is presented for each system with experimental data provided to demonstrate the performance of each system. Both systems described herein maximize component reuse and fully integrate transmit and receive modes in efficient hardware compressive topologies.

**14. SUBJECT TERMS**

phased array antennas, true time delay beamforming, broadband microwave signals, broadband null steering, photonics, fiber bragg reflective gratings, high dispersion optical fiber

**15. NUMBER OF PAGES**

56

**16. PRICE CODE**

| 17. SECURITY CLASSIFICATION OF REPORT | 18. SECURITY CLASSIFICATION OF THIS PAGE | 19. SECURITY CLASSIFICATION OF ABSTRACT | 20. LIMITATION OF ABSTRACT |
|---|---|---|---|
| UNCLASSIFIED | UNCLASSIFIED | UNCLASSIFIED | UL |

# Abstract

Several relatively new photonic components have recently come to the forefront in applications related to the photonic processing of broadband microwave signals. Included in this set of photonic elements are the wavelength tunable laser, high dispersion optical fiber, and the Bragg reflection grating. These components hold the promise of revolutionizing the field of broadband photonic processing. This report documents the performance characteristics of these components and shows how they can be used for two broadband phased array applications, beamforming and null steering. Two systems are described. A technical overview is presented for each system with experimental data provided to demonstrate the performance of each system. Both systems described herein maximize component reuse and fully integrate transmit and receive modes in efficient hardware compressive topologies.

# Table of Contents

# List of Figures

# List of Tables

# Preface

The purpose of this final report is to document all work associated with the Air Force Research Laboratory in-house project 4600P137. The report documents two distinctive phased array beamforming architectures that enable wideband operation. The architectures are both based on photonic techniques for generating true time delay (TTD) to enable wideband operation.

# Acknowledgements

Mr. Paul Payson, of AFRL, constructed, tested and analyzed the photonic breadboard system for the Fiber Grating Prism beamformer. Additionally, Mr. Payson developed, designed, constructed, tested and analyzed the high dispersion optical fiber nulling system.

Dr. Henry Zmuda, of the University of Florida, designed, constructed, tested and analyzed the photonic breadboard system for the Fiber Grating Prism beamformer. Additionally, Dr. Zmuda developed the theory for, developed, designed, constructed, tested and analyzed the high dispersion optical fiber nulling system.

Dr. Edward Toughlian, of ENSCO Inc., developed the theory for, designed, and analyzed the high dispersion optical fiber nulling system.

Mr. Richard Soref, of AFRL, developed the theory and architecture for the Fiber Grating Prism beamformer.

Mr. Herbert Klumpe, III, of AFRL, constructed, and tested the high dispersion optical fiber nulling system.

Mr. Steve Johns, of AFRL, constructed the photonic breadboard system for the Fiber Grating Prism beamformer.

# List of Abbreviations and Acronyms

| | |
|---|---|
| AF | Array Factor |
| AGC | Automatic Gain Control |
| BRG | Bragg Reflective Grating |
| COTS | Commercial Off the Shelf |
| DBR | Distributed Bragg Reflector |
| DFB | Distributed Feedback |
| EMI | Electro Magnetic Interference |
| EMP | Electro Magnetic Pulse |
| EOM | Electro-Optic Modulator |
| FGP | Fiber Grating Prism |
| FSR | Free Spectral Range |
| FWHM | Full Wave Half Maximum |
| GPS | Global Positioning System |
| HDOF | High Dispersion Optical Fiber |
| LNA | Low Noise Amplifier |
| nm | nanometer |
| OI | Optical Isolator |
| PC | Polarization Controller |
| PD | Photodetector |
| ps | picosecond |
| SAW | Surface Acoustic Wave |
| SFDR | Spur Free Dynamic Range |
| SRE | Signal Routing Element |
| TLS | Tunable Laser Source |
| TTD | True Time Delay |

| | |
|---|---|
| UV | Ultraviolet |
| WDM | Wavelength Division Multiplexing |
| WML | Wavelength Multiplexed Laser |

# 1.0 Introduction

The use of dynamic techniques to electronically steer the aperture of a phased array antenna system has been a topic of great interest. A phased array has the ability to focus beams in specified spatial coordinates while simultaneously placing nulls along other spatial coordinates making it immune to jammers, intentional or otherwise, and providing a significant reduction in multi-path interference — a problem of great concern in most communications applications.

Electronic processing systems that accomplish beamsteering have a distinct set of limitations. Microwave circuit components tend to be cumbersome, especially at lower microwave frequencies. This has limited the widespread use of large phased arrays, especially in airborne applications where size and weight are primary concerns. Another significant problem is that the microwave circuit components needed to implement a beamformer are inherently narrowband, limiting the bandwidth of the beamforming system to a few percent of the RF carrier frequency. The use of narrowband components results in a beam pointing error known as *squint*, where each frequency component points in a different spatial direction. Since future communication and surveillance systems require wideband performance (2-18 GHz for surveillance systems and up to 50 GHz for communications systems), a new method is needed to remove squint and these other current limitations.

To eliminate squint error, phased arrays must employ true-time delay (TTD) beamforming techniques. The antenna is "steered" by applying an appropriate amount of time delay to each signal used to drive the elements of the array. The only way to achieve time-delay of a microwave signal — short of digitizing it and storing it in a computer memory for later re-construction — is to provide an appropriate path length for the signal

to propagate. Reconfigurable beamsteering requires a variable length line; the practical implementation of which has been a challenging problem.

In recent years, optical processing techniques for microwave signals have made significant advances in the area of phased array antenna control[1]. Several advantages of optical processing techniques are often touted, such as reduced weight and increased immunity to Electro Magnetic Pulse (EMP) and Electro Magnetic Interference (EMI) effects. Yet beyond these advantages, perhaps the greatest contribution of optical processing techniques for phased arrays will be its ability to incorporate true-time delay beamforming methods in some rather innovative ways. Recent developments in both in-fiber optical components and optical integrated circuits have led to optically controlled phased array architectures which could provide a field-worthy system in the short term. Developments in tunable wavelength laser technology allow systems utilizing high dispersion optical fiber to achieve a variable microwave delay line[2,3,4]. Recent advances in fabricating permanent fiber-based Bragg reflection gratings (BRGs) have made these devices off-the-shelf products[5,6]. BRGs show great promise for microwave delay line technology and have been

---

[1] H. Zmuda and E.N. Toughlian, *"Photonic Aspects of Modern Radar,"* Boston: Artech House, 1994.

[2] M.Y. Frankel and R.D. Esman, *"True Time-Delay Fiber-Optic Control of an Ultrawideband Array Transmitter/Receiver with Multibeam Capability,"* IEEE Transactions on Microwave Theory and Techniques, Vol. 43, No.9, pp. 2387-2394, September 1995.

[3] S.T. Johns, D.A. Norton, C.W. Keefer, R. Erdmann, and R.A. Soref, *"Variable Time Delay of Microwave Signals Using High Dispersion Fiber,"* Electronics Letters, Vol. 29, No. 6, pp. 555-556, 18 March 1993.

[4] R.A. Soref, *"Optical Dispersion Technique for Time-Delay Beam Steering,"* Applied Optics, Vol. 31, No. 35, pp. 7395-7397,10 December 1992.

[5] R.J. Campbell and R. Kashyap, *"The Properties and Applications of Photosensitive Germanosilicate Fiber,"* International Journal of Optoelectronics, Vol. 9, No. 1, pp. 33-57, 1994.

[6] M.C. Farries, K. Sugden, D.C.J. Reid, I. Bennion, A. Molony, and M.J. Goodwin, *"Very Broad Reflection Bandwidth (44nm) Chirped Fiber Gratings and Narrow Bandpass Filters Produced by the use of an Amplitude Mask,"* Electronic Letters, Vol. 30, No. 11, pp. 891-892, 1994.

proposed for use in phased array transmit/receive systems[7,8,9,10]. These systems are fiber-based and therefore have the distinct advantage of being able to incorporate fiber amplifiers; allaying some of the concerns of a single laser source being distributed to the (potentially) many channels of a phased array system.

This report documents two innovative architectures for phased array antenna beamforming. One generates time delay discretely using BRGs and a tunable optical source. The second architecture generates a continuum of time delays utilizing a high dispersion optical fiber (HDOF) and several tunable optical sources. The variable true-time-delay beamformer is especially useful for null steering applications.

---

[7] G.A. Ball, W.H. Glenn and W.W. Morey, *"Programmable Fiber-Optic Delay Line,"* IEEE Photonics Technology Letters, Vol. 6, No. 6, pp. 741-743, June 1994.

[8] A. Moloney, C. Edge, and I. Bennion, *"Fiber Grating Time Delay Elements for Phased Array Antennas,"* Electronics Letters, Vol. 31, No. 17, pp. 1485-1486, 17 August 1995.

[9] R.A. Soref, *"Fiber Grating Prism for True Time Delay Beamsteering,"* Fiber and Integrated Optics, Vol. 15, No. 4, pp. 325-333, October 1996.

[10] H. Zmuda, R.A. Soref, P. Payson, S. Johns, and E.N. Toughlian, *"Photonic Beamformer for Phased Array Antennas Using a Fiber Grating Prism,"* IEEE Photonics Technology Letters, Vol. 9, No. 2, pp. 241-243, Feb. 1997.

# 2.0 Background

## 2.1 Theory of Phased Array Beamforming

To gain a general understanding of the operation of a phased array system, consider a linear array of equally spaced isotropic point sources and determine its radiation pattern or array factor *(AF)*[11]. Start by considering the far field radiation pattern. The incoming rays from a point source in the far field can be approximated as traveling parallel to one another by the time they reach the antenna array. This approximation allows for the concise analytical expression of the *AF*. The approach taken to find an analytical expression for the *AF* is to first consider the receive mode of operation. From Figure 1 we find the *AF* by summing the far field excitation of all the elements.

$$AF = I_o + I_1 e^{j\beta d \sin\theta} + I_2 e^{j\beta 2d \sin\theta} + \ldots = \sum_{n=0}^{N-1} I_n e^{j\beta nd \sin\theta} \tag{1}$$

N is the total number of elements in the array, $n=0, 1, \ldots, N-1$ is the element number, $d$ is the Spacing between elements, $\beta$ is the propagation constant in free space, $I_n$ is the received element current, and $\theta$ is the observation or measurement angle.

Since an antenna is a reciprocal device, we can immediately see how to steer a transmitted beam to a desired angle $(\theta_0)$, simply by forcing all the rays to travel the same path length to reach the desired location in the far field.

[11] W.L. Stutzman, G.A. Theile, *"Antenna Theory and Design,"* John Wiley and Sons, 1981.

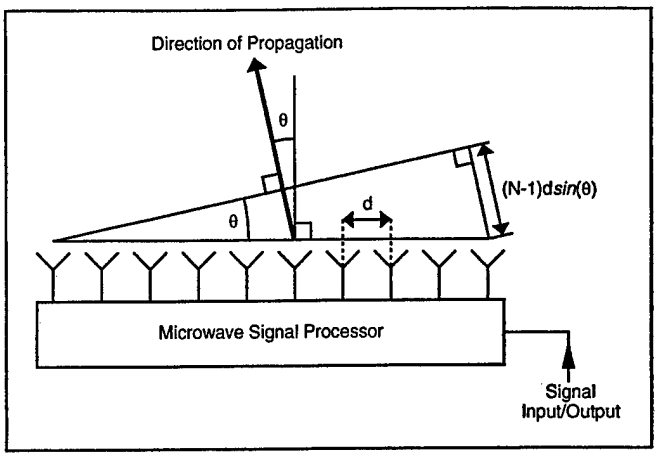


Figure 1. A steered phased array antenna.

The *AF* can be written as:

$$AF = \sum_{n=0}^{N-1} I_n e^{j(\beta nd \sin\theta + \beta_L L_n)} \tag{2}$$

$L_n$ is the physical length of the line used to delay the signal at element $n$, and $\beta_L$ is the propagation constant for the line. This is the same condition as requiring the relative phase between elements to be zero in the far field at the desired steer angle.

Therefore, we find the incremental delay line length *(L)* from:

$$0 = \beta nd \sin\theta_o + \beta_L L_n \tag{3}$$

Therefore:

$$L_n = -\frac{\beta}{\beta_L} nd \sin\theta_o \tag{4}$$

Of course, more complicated radiation patterns can be achieved by applying other than a linear phase progression across the array.

We are now at a point where we can distinguish between phase shift and true time delay beam steering techniques. The differential phase ( $\Delta\phi$ ) between elements for a linear phase progression between elements can be written:

$$\Delta\phi(\omega) = \beta_L \Delta L = \omega T \tag{5}$$

$T = \frac{\Delta L}{\upsilon}$ is the time delay of the line, $\Delta L = \frac{-\beta}{\beta_L} d \sin\theta_o$ is the differential line length between elements, and $\upsilon$ is the signal velocity of propagation in the line. When all frequencies see the same time delay, as is the case for the system described by Equation (5), the system is said to be of the true time delay type. Also, from Equation (5), it should be noted that for the true time delay system, the phase is a linear function of frequency with a slope of $T$.

The phase shift implementation is accomplished by setting the differential phase equal to a constant, typically:

$$\Delta\phi = \omega_c T \tag{6}$$

$\omega_c$ is the center frequency of the band to be radiated. In other words, all frequency components receive the same phase shift. The energy associated with the center frequency radiates in the desired direction. However, the energies of the other frequency components radiate in other directions centered about the desired direction.

## 2.2 Beamsquint

Beamsquint is a phenomenon, where the energy associated with the different frequencies focuses in different directions in the antenna's far field. For a wide bandwidth system this phenomena shows up as an increase in beam width. True time delay systems generate

properly phased signals theoretically eliminating beamsquint, thus enabling wide bandwidth operation. In the following section the beamsquint problem of a conventional phase shift radar system is described.

At the $N^{th}$ element of a linear array the phase may be described as follows:

$$\phi = \frac{2\pi N d}{\lambda} \sin\theta \tag{7}$$

$\lambda$ is the wavelength of the design transmit frequency, $d$ is the element spacing (for our system $\lambda/2$) and $\theta$ is the angle of the wavefront as measured from the plane of the linear array.

Rewriting the equation gives:

$$\sin\theta = \frac{\phi\lambda}{2\pi N d}. \tag{8}$$

For an incremental change in frequency the equation becomes:

$$\frac{\partial}{\partial\lambda}\sin\theta = \frac{\partial}{\partial\lambda}\frac{\phi\lambda}{2\pi N d}. \tag{9}$$

or

$$\cos\theta\frac{\partial\theta}{\partial\lambda} = \frac{\phi}{2\pi N d}. \tag{10}$$

Solving for $\partial\theta$ and substituting using Equation (8) gives:

$$\partial\theta = \frac{\partial\lambda}{\lambda}\tan\theta. \tag{11}$$

Therefore

$$\partial\theta = \frac{\partial f}{f}\tan\theta \tag{12}$$

or the beamsquint $(\Delta\theta)$ is given by:

$$\Delta\theta = -\frac{\Delta f}{f}\tan\theta \tag{13}$$

The negative sign is added to indicate that as frequency increases the scan angle decreases from the center frequency.

The relationship described in Equation (13) has some interesting ramifications. The aperture size and the beam width have no influence on the beamsquint. As frequency increases the scan angle decreases. Perhaps most significantly, the frequency sensitivity depends on the boresight angle θ. Beamsquint increases as the steer angle increases (gets further away from broad side)[12].

[12] A. Oliner, G Knittel, *"Phased Array Antennas,"* Artech House, Massachusetts, 1972.

# 3.0 Enabling Technologies

## 3.1 High Speed Tunable Laser Technology

As seen in the introduction, both the discrete and continuous TTD architectures developed require tunable optical sources. Application to phased array antenna systems requires these critical components to be broadly tunable [10-50 nanometer (nm)] and high speed (>1 MHz). Unfortunately, commercial-off-the-shelf(COTS) devices meeting such requirements are not readily available. However, the telecommunications industry's recent interest in the application of photonic processing methods for wavelength division multiplexing (WDM) systems has led to a proliferation in research of tunable laser technology. Trends in WDM communication indicate that a broadly tunable laser capable of random wavelength access will play a key role in future systems. Current research in both tunable lasers and tunable filters being developed by the telecommunications industry offers substantial promise that our system requirements will be met. The following briefly synopsizes some of the various approaches for developing tunable devices.

Semiconductor lasers consist of an active gain medium that is spectrally broad and that defines the free spectral range (FSR) over which the laser may be frequency tuned. A cavity structure containing a wavelength selective element establishes the operating wavelength of the laser. Several methods exist for modifying the operating wavelength via modulation of the wavelength selective element. One approach is by rapidly varying the index of an etalon contained within the cavity. This type of electro-optic tuning is range limited to < 2 THz (16 nm at a 1.55 μm center wavelength) since only small index changes are possible. Mechanical tuning is another approach which can achieve extremely broad tuning ranges but is generally very slow (kHz ~ low MHz range). Large, rapid wavelength

variation may be obtained by modulating the angle at which the light travels in the cavity thereby changing the physical path length. This angle modulation can be performed with a variety of beam deflection techniques ranging from electro-optic beam deflectors to acousto-optic deflectors or surface acoustic wave (SAW) devices. Such devices can operate at multi-gigahertz rates[13]. One fiber-laser based approach uses acousto-optic tunable filters to achieve rapid, broad range tuning[14].

Other approaches include externally addressable Fabry-Perot devices and birefringent tuning via Pockel cells. Mach-Zehnder based Y-branch lasers are capable of rapid wide-band tuning with a single control current[15]. Distributed Bragg Reflector (DBR) lasers are passively tuned and have a continuous or discrete tuning range of about 10 nm, limited by carrier lifetimes[16]. Distributed Feedback (DFB) lasers have an active tuning region that result in much shorter carrier lifetimes. Tuning speeds of less than one nanosecond are possible but at the expense of a smaller tuning range[17]. Both the DBR and DFB lasers rely on the fractional index change from the electro-optic effect to tune.

Attempts to obtain broad tuning at high speed are being pursued by several researchers. Laser structures such as Vertical Grating Assisted Coupler lasers can currently achieve a

---

[13] P. Zoribedian, "*External Cavity Tunable Lasers,*" in: A.J. Duarte, Editor, Tunable Laser Technology, New York: Academic Press, 1995.

[14] M.Y. Frankel, R.D. Esman, and J.F. Weller, "*Rapid Continuous Tuning of a Single-Polarization Fiber Ring Laser,*" IEEE Photonics Technology Letters, Vol. 6, No. 5, pp. 591-593, May 1994.

[15] M. Kuznetsov, "*Design of widely tunable semiconductor three branch lasers,*" IEEE Journal of Lightwave Technology, Vol. 12, No. 12, pp. 2100-2106, Dec. 1994.

[16] B. Glance, U. Koren, C.A. Burrus, J.D. Evankov, "*Discretely-Tuned N-Frequency Laser for Packet Switching Applications Based on WDM,*" Electronics Letters, Vol. 27, No. 15, pp. 1381-1383, 18 July 1991.

[17] M. Morinaga, M. Ishikawa, and N. Suzuki, "*Analysis on Wide Continuous Wavelength Tuning of Rapid-Tunable Quantum-Well DFB Lasers with Carrier-Transport Effects,*" IEEE Journal of Selected Topics in Quantum Electronics, Vol. 1, No. 2, pp. 427-432, June 1995.

tuning range of 50 nm with larger ranges expected[18]. Super Structure Grating DBR lasers can currently achieve 100 nm tuning[19]. Both these technologies can currently tune at rates of less than 10 nanoseconds. Another way to overcome the conflict between switching time and tuning is to switch among laser diodes with a high-speed switching matrix. One such approach implemented for WDM applications utilizes electro-absorption optical switching to achieve a wavelength switching time of about 10 Picosecond (ps)[20].

## 3.2 Bragg Reflection Grating (BRG)

An integral component of the photonic TTD systems presented in this paper is the BRG. Recent advances in BRG technology coupled with efficient manufacturing methods have allowed the BRG to become a COTS product[21]. Reflection gratings are generally made by exposing a hydrogen-loaded silica fiber to a periodic pattern produced by either a mask or an interference pattern using an intense ultraviolet (UV) laser. This exposure causes a periodic phase grating to be permanently written into the core and cladding of the fiber. For wavelengths within the transmission stop band, the grating couples energy from the incident wave into the corresponding reflected wave. The magnitude of the UV induced index deviation and the length of the grating — which are readily controlled design parameters — determine the BRGs spectral bandwidth and reflectivity. Devices with re-

---

[18] Y. Tohmori, F. Kano, H. Ishii, Y. Yoshikuni, and Y Kondo, "*Wide Tuning with Narrow Linewidth in DFB Lasers with Superstructure Grating (SSG),*" Electronic Letters, Vol. 29, No. 15, pp. 1350-1351, 22 July 1993.

[19] I. Kim, R.C. Alferness, U. Koren, L.L. Buhl, B.I. Miller, M.G. Young, M.D. Cohen, T.L. Kock, H.M. Presby, G. Raybon, and C.A. Burrus, "*Broadly Tunable Vertical-Coupler Filtered Tensile-Strained InGaAs/InGaAsP Multiple Quantum Well Laser,*" Applied Physics Letters, Vol. 64, No. 21, pp. 2764-2766, 23 May 1994.

[20] H. Okamoto, H. Yasaka, K. Sato, Y. Yoshikuni, K. Oe, K. Kishi,. Y. Kondo, and M. Yamamoto, "*A Wavelength-Tunable Duplex Integrated Light Source for Fast Wavelength Switching,*" IEEE Journal of Lightwave Technology, Vol. 14, No. 6, pp. 1033-1041, June 1996.

[21] R.J. Campbell and R. Kashyap, "*The Properties and Applications of Photosensitive Germanosilicate Fiber,*" International Journal of Optoelectronics, Vol. 9, No. 1, pp. 33-57, 1994.

flection bandwidths as narrow as 0.02 nm or as broad as 100 nm are available from several manufacturers. Broad reflection bandwidths are obtained using a chirped rather than a periodic index variation[22]. Reflectivity at the Bragg wavelength can be designed to be as low as 1% or greater than 99.9%. Off-wavelength transmission is nearly 100%. Consequently, BRGs are an extremely efficient and versatile optical design element.

## 3.3 High Dispersion Optical Fiber (HDOF)

As alluded to in the introduction, one of the photonic TTD architectures presented here uses HDOF in conjunction with a tunable optical source to generate a continuum of time delays. Due to a phenomenon called chromatic dispersion, the group velocity associated with the fundamental mode is frequency dependent. The frequency dependence of the group velocity leads to pulse broadening because different spectral components disperse during propagation and become desynchronized at the fiber output[23]. Dispersion (D) is expressed in units of ps/(km-nm). HDOF possesses enhanced chromatic dispersion relative to other single mode fibers [$D_{HDOF} \approx 100$ ps/(km-nm) and $D_{smf} \approx 10$ ps/(km-nm) @ 1550 nm].

[22] M.C. Farries, K. Sugden, D.C.J. Reid, I. Bennion, A. Molony, and M.J. Goodwin, *"Very Broad Reflection Bandwidth (44nm) Chirped Fiber Gratings and Narrow Bandpass Filters Produced by the use of an Amplitude Mask,"* Electronic Letters, Vol. 30, No. 11, pp. 891-892, 1994.

[23] G.P. Agrawal, *"Fiber Optic Communication Systems,"* John Wiley & Sons, pp. 39-41, 1992

# 4.0 Discrete TTD Fiber Bragg Reflective Grating (BRG) Beamforming System

## 4.1 System Description

This section describes a photonic beamformer that generates time delay discretely using BRGs in conjunction with a tunable laser source (TLS). The system level diagram for the beamformer is shown in Figure 2. For the transmit mode of operation one TLS is externally modulated with an electro-optic modulator (EOM). This modulated light feeds a group of N single-mode fibers through an equal-path (1:N) power divider. The EOMs used for receive are not used for transmit. Optical circulators direct the modulated signals to the Fiber Grating Prism (FGP). Each fiber includes a spatially distributed array of BRGs that collectively form the FGP. The different peak-reflection wavelengths $\lambda_1$ ... $\lambda_M$ of the various gratings are within the tuning range of the laser $\Delta\lambda$. The 1:N splitter includes an N-fold set of integrated 3 dB directional couplers that gather the back-traveling light from the wavelength-selective gratings. Reflected light is time-delayed in accordance with the particular grating addressed. For the transmit mode, a second set of equal-length fibers transports the N coupler outputs to a set of spectrally broad photodetectors (PD) located at the array which recover the delayed microwave signals that feed the antenna-radiator elements. In the receive mode an unmodulated TLS feeds N optical channels as above. The received microwave signals are directed to a set of N EOMs. The modulated optical signals are then directed to the FGP via the optical circulators. These optical signals are summed together and sent to a PD for recovery of the collective microwave signal. Wavelength shift in the TLS selects a desired outgoing as well as incoming beam direction.

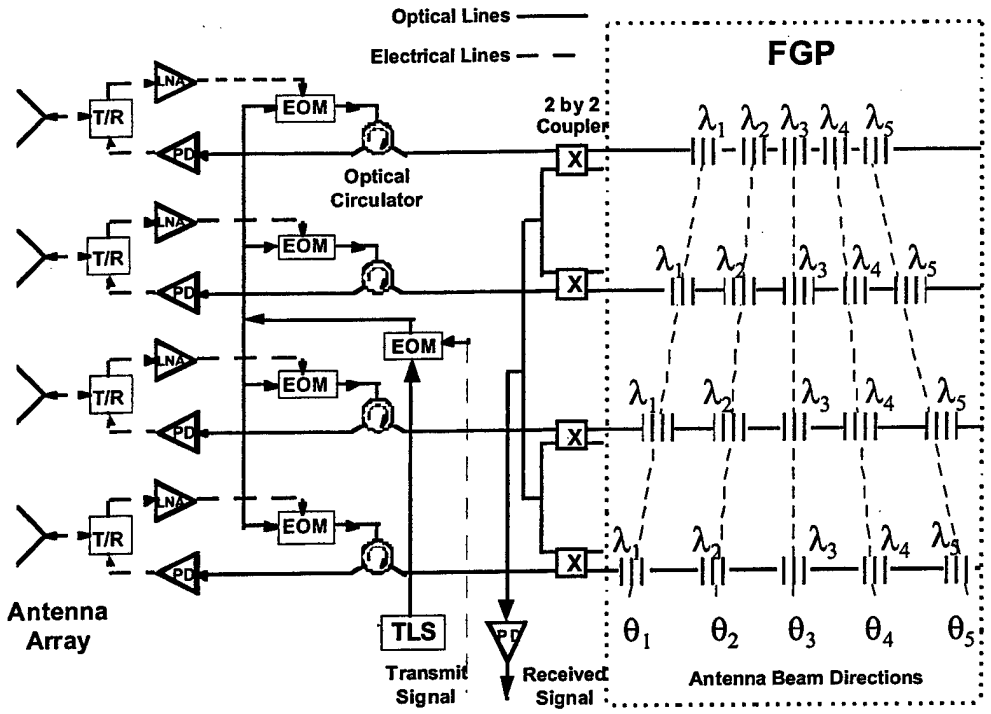


Figure 2. Fiber Grating Prism TTD transmit/receive architecture.

Figure 2 also illustrates the spatial layout of the fiber prism's Bragg gratings for the case of N = 4. Here, the main lobe of the phased-array antenna can point in any one of five discrete directions (M = 5) as selected by the laser wavelength. The dashed lines in the FGP region of the figure show the progressive separation of neighboring gratings, within a fiber, and from fiber to fiber.

To understand the basic design details of the FGP circuit, we assume an array of uniformly spaced radiators a distance $s$ apart. A plane wave will propagate from the array (in the far field) in a direction $\theta_i$ (measured with respect to broadside) when a differential time delay $\Delta t_i = (s/c_o) \sin \theta_i$ is established between adjacent radiators ($c_o$ is the speed of light in free space). The FGP provides the desired group of differential delays $T_{ij}$ by a set of double pass delays to-and-from the next grating: $T_{ij} = 2d_{ij}n/c_o$, where $d_{ij}$ is the spacing between the center of the $i^{th}$ grating in fiber j and the center of the broadside grating in fiber

j, n is the fiber waveguide index *(n≈ 1.5)*, i = 1, 2, 3, ..., M and j = 1, 2, 3, ..., N. A critical design parameter is the minimum steer angle step size $\theta_{min}$ which dictates the minimum grating spacing $d_{\min}$ . It has been shown that $\theta_{min} = \arcsin(4nf_m d_{\min}/c_o)$ where $f_m$ is the maximum microwave frequency and $d_{\min} = d_{21}$ and that the number of resolvable beam positions is $r = c_o\Delta\lambda/3f_m\lambda_o^2\sin(\theta_{\min})$ where $\Delta\lambda$ is the laser's tuning range and $\lambda_o$ is the central wavelength of the laser [7]. Limits on how closely the BRGs can be spaced on a fiber determines the number of usable beam positions. A typical number is 50% to 100% of *r*. In situations where the spacing between grating becomes less than the grating length, there may be a problem resolving adjacent delays due to optical crosstalk. We estimate that the minimum practical grating spacing is one-half of the grating length.

Regarding system loss, the laser power reaching the PDs in Figure 2 is reduced by several factors in both transmit and receive mode of operation. The FGP introduces a loss 1 - *R*, where *R* is the reflectance of the selected grating. The reflectance of the BRGs can be greater than 99%, while the M - 1 unselected gratings per channel do not introduce appreciable optical loss, typically less than 0.4 dB. The major loss mechanisms are the couplers (6 dB per round trip), the 1:N splitter/summer (10 log N dB), and the circulator (1 dB per direction). Note that the receive mode experiences additional loss due to a second splitter. Generally, an EOM biased at quadrature contributes a total insertion loss of approximately 6 to 8 dB. Note also that in the receive mode, EOM used for transmit, is not used, and vice versa. Splices, connectors, isolators, polarization control, and the like will add another few dB of excess loss to the system. Detector responsivity will generally provide gain. The total loss is the sum of the above, and the RF loss is twice the optical loss. Since the system is fiber-based, optical amplifiers can be incorporated into the design to compensate for the insertion losses in the system. It is also necessary to maintain uniform amplitude among the various wavelength-channels so that the amplitudes track for all steer angles. Experimentally the dc biases of discrete wavelength lasers were

adjusted to give equal optical amplitudes. In a practical antenna system driven by the single tunable laser in Figure 2, some amplitude errors will inevitably arise during the wavelength scanning, but those variations can be compensated for at the antenna plane by an equalization method in the electronic domain. The equalization technique is to adjust the electrical bias of each preamplifier following each PD [and the bias of each Low Noise Amplifier (LNA)] so that the detected microwave signal has the same amplitude at each antenna element. Post-detection electronics such as amplification, impedance matching automatic gain control (AGC) circuitry, etc., is present with any phased array antenna and its inclusion here does not add to the complexity of the beamforming network presented.

## 4.2 Experimental Set-Up

Figure 3 shows our experimental system, constructed for the case of a linear array with N=3 and, M=1. The FPG was designed to steer a three-element aperture to four positions: 0°(broadside), 30°, 59°, and 60°. Each of three single mode fibers contained a series of four Bragg gratings manufactured by 3M corporation. The peak grating reflection had spectral widths [Full Wave Half Maximum (FWHM)] of 0.2 nm. The peak reflection wavelengths of the grating trios were 1552, 1553, 1557, and 1560 nm, respectively with the reflectivity of each greater than 70%. The individual gratings were 6.45 mm long ($L_g$ in Figure 3). These fiber gratings were fed by an optical equal-arm "tree" splitter consisting of three 2 x 2 fused-fiber 3 dB couplers, $c_1$, $c_2$, and $c_3$. The spatial location $d_{ij}$ of grating i along fiber j was as follows: $d_{11} = 0$, $d_{21} = 1.72$ cm, $d_{31} = 4.67$ cm, $d_{41} = 7.65$ cm, $d_{12} = 0$, $d_{22} = 3.44$ cm, $d_{32} = 7.62$ cm, $d_{42} = 10.63$ cm, $d_{13} = 0$, $d_{23} = 5.16$ cm, $d_{33} = 10.57$ cm, and $d_{43} = 13.61$ cm. This prism-shaped layout is shown in Figure 3. The optical return signals were routed by 3 dB fiber couplers $c_4$, $c_5$ and $c_6$ as shown, and directed to a spectrally broad Hewlett-Packard *model 11983* p-i-n lightwave converter (PD). Optical circulators were not used. Four thermally tunable diode lasers manufactured by Sea Star Inc., oper-

ating at 1552, 1553, 1557, and 1560 nm, were multiplexed on one optical feed to simulate one broadly tunable laser source (WML = Wavelength Multiplexed Laser). An AT&T model M2122AA Ti:$LiNbO_3$ Mach-Zehnder amplitude modulator (EOM) was used to modulate the optical carrier with an RF signal whose frequency varied from 500 MHz to 4GHz. The EOM RF port was driven by a Hewlett-Packard *model 8753* 6 GHz network analyzer. Our breadboard system included a polarization controller (PC) for the EOM, and an optical isolator (OI) at the WML output. The p-i-n detector output was fed into Port 2 of the Network Analyzer, which was used to gather time-delay data. Calibration of the measurement system, consisting of all of the above components except for the FGP was performed on the network analyzer and delay data was gathered using 201 samples over the 3.5GHz bandwidth with no averaging.

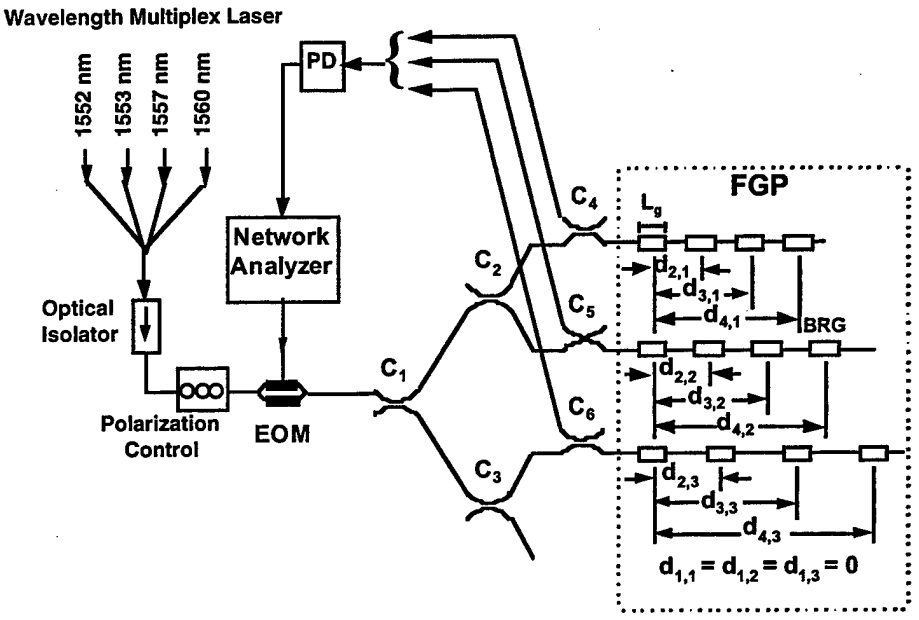


Figure 3. Fiber Grating Prism TTD beamforming experimental set up.

## 4.3 Discussion of Experimental Results

Figure 4 shows the measured time delay data (phase vs. frequency) for the FGP. The FGP was designed to steer the mainlobe to angles of 30°, 59°, and 60°. Obviously this 3 element system requires 3 time delays per steer angle. The measured delays were a bit off the design goals due to positioning accuracy (or lack there of) of the BRGs on the fiber (see Table 1). These positioning inaccuracies caused the actual steer angle to differ from our design goal.

Table 1. Measured vs. designed delays.

| Designed Time Delay (ps) | Designed Steer Angle(degrees) | Measured Steer Angle(degrees) | Measured Time Delay (ps) |
|---|---|---|---|
| 166.7 | 30 | 33.25 | 172.0 |
| 333.3 | 30 | 33.25 | 332.3 |
| 500 | 30 | 33.25 | 534.2 |
| 452.4 | 59 | 67.5 | 427.2 |
| 738.1 | 59 | 67.5 | 719.3 |
| 1023.8 | 59 | 67.5 | 1043.9 |
| 741.06 | 60 | 67.9 | 740.1 |
| 1029.9 | 60 | 67.9 | 1030.57 |
| 1318.4 | 60 | 67.9 | 1353.9 |

Figures 5, 6, and 7 show the actual steer angles to be 33.25°, 67.5° and 67.9°. Budgetary limitations dictated that the tolerance on the positioning of $d_{ij}$ be held to ± 1mm or about 3%. In a final, fully engineered system, current BRG manufacturing technology can reduce this positioning error to as small a value as is necessary. Figure 8 shows a zoomed in

view of the main lobe of Figure 5. From Figure 8 we see that there is little if any beamsquint as all three frequencies (1.515 GHz, 2.5125 GHz, and 3.5 GHz) radiate in the same direction. Figure 9 shows how beamsquint would effect a phase shift system. We see that for a phase shift system with a design frequency (where the inter-element spacing $d=\lambda/2$) of 1.5 GHz and a desired steer angle of 30°, the beamsquint would be approximately 20° at 2.5 GHz and 40° at 3.5 GHz. The beamsquint would increase for larger steer angles [refer to Equation (13)].

The Spur Free Dynamic Range (SFDR) is determined in the conventional way via SFDR (dB) = $(2/3)[IP_3 - N_o]$. Where, $IP_3$ is the third-order intercept point (in dBm), $N_o$ is the total output noise and includes the effects of thermal noise, noise figure, and total system gain. The information for the noise figure was obtained using a noise figure test set, and each leg of the FGP had a typical noise figure of 20 dB on average over the 3.5GHz band. Measured data for third order intermodulation products showed a SFDR of 42 dB/Hz. Measurements indicate that the dominant phase noise and nonlinear effects are due to the EOM as expected. The nominal phase noise (seen in the insert in Figure 4) shows a rms phase error of less than one degree over the 3.5GHz band, a result superior to any comparable electronic beamsteering system. The measured spurious-free dynamic range (SFDR) should not be interpreted as best case, since a final, fully engineered system would likely perform much better than the breadboard system measured here. For example, the AT&T modulator has an impedance measuring 43Ω, which resulted in amplitude variations due to mismatch effects.

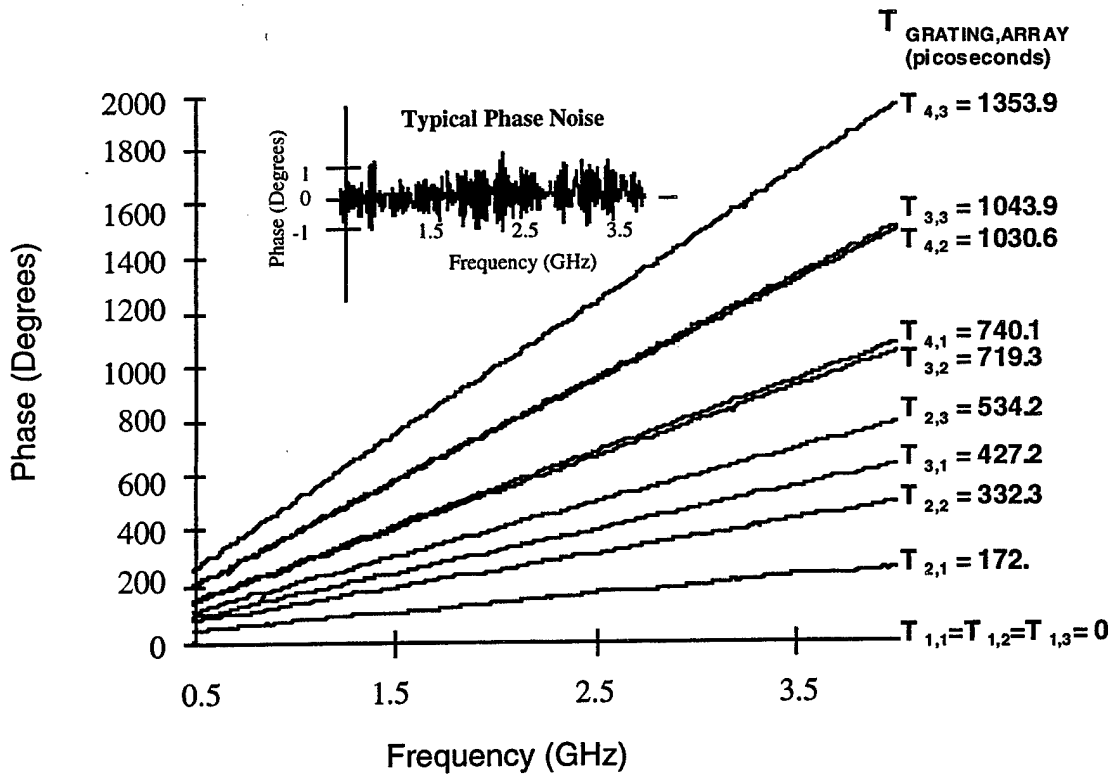


Figure 4. Delay vs. Frequency for Fiber Grating Prism beamforming breadboard.

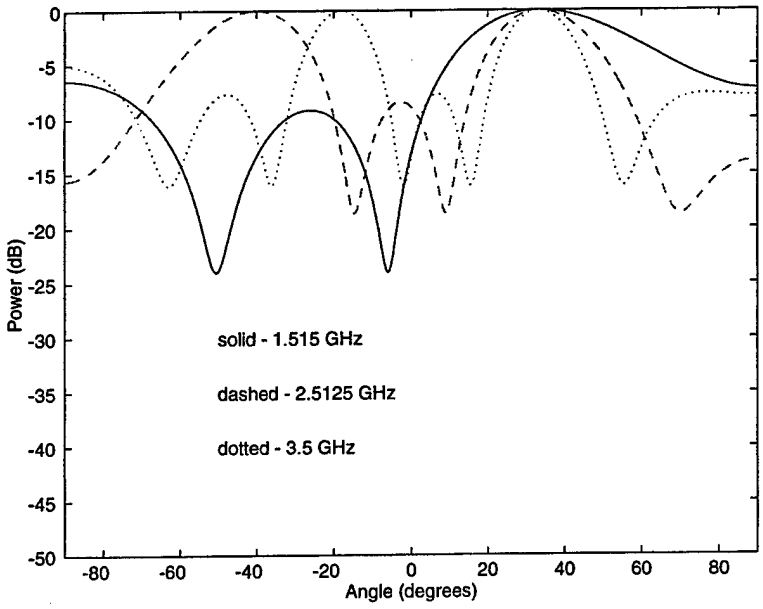


Figure 5. Array Factor for 30° design steer angle, 33.25° actual steer angle.

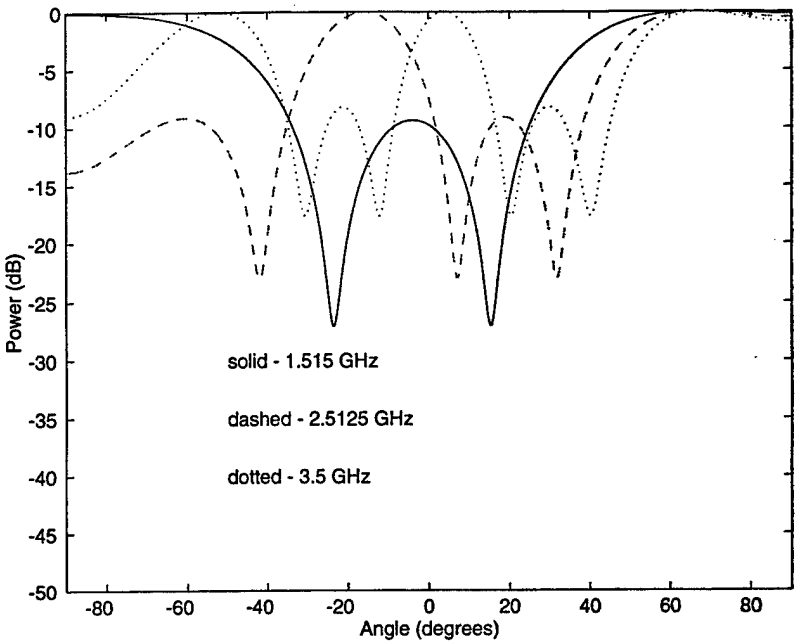


Figure 6. Array Factor for 59° design steer angle, 67.5° actual steer angle.

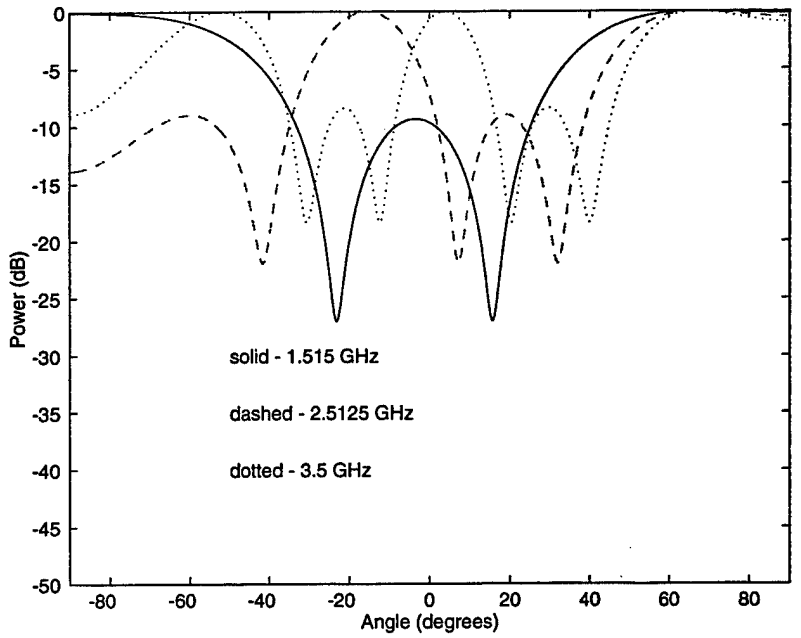


Figure 7. Array Factor for 60° design, 67.5° actual steer angle.

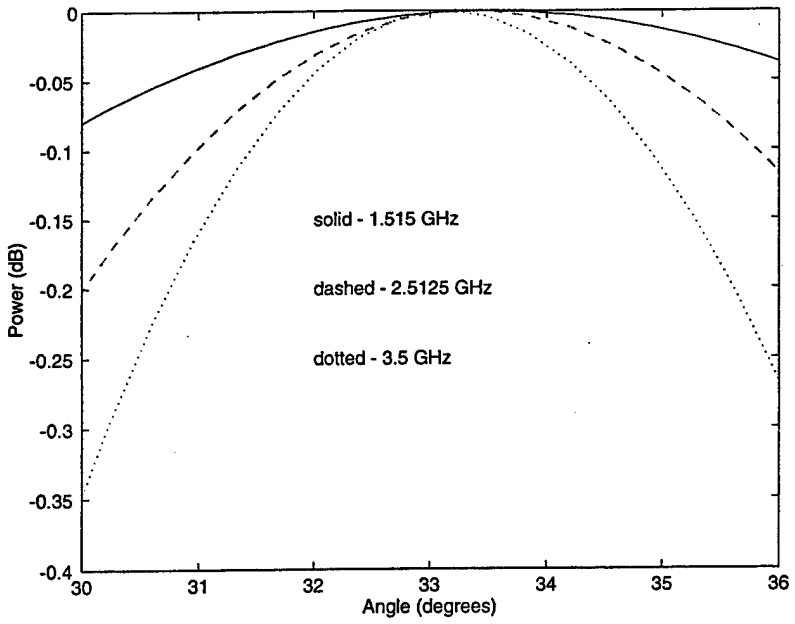


Figure 8. Array Factor for 30° design steer angle, 33.25° actual steer angle. Zoomed in to show how the TTD beamformer overcame squint.

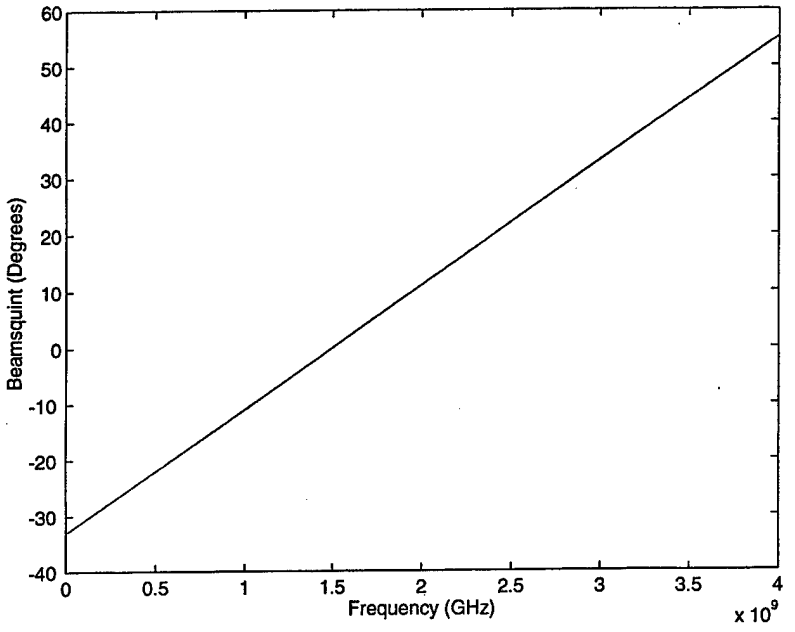


Figure 9. Beamsquint for a phased array with a design frequency=1.5 GHz and a desired steer angle of 30°.

# 5.0 Continuously Variable TTD High Dispersion Optical Fiber (HDOF) Beamforming System

## 5.1 System Description

This section describes a photonic beamformer that generates a continuum of time delays using HDOF in conjunction with tunable laser sources[24,25,26](TLS). A microwave signal used to modulate an optical carrier with wavelength $\lambda$ will undergo a time delay of

$$\tau(\lambda) = D \cdot \lambda \cdot \ell \tag{14}$$

where D is the dispersion (in units of psec/km-nm) and $\ell$ is the length of the HDOF. The system can be used as a phased array antenna beamformer in both transmit and receive mode.

Figure 10 shows an integrated transmit/receive continuously variable TTD beamformer that obtains the time delay from HDOF and uses BRGs for a wavelength demultiplexing. Transmit operation is examined first. The figure shows a set of N modulated tunable wavelength lasers, each operating at a distinct wavelength $\lambda_j$ , j = 1, ... , N. Each of these lasers is coupled to a fixed length of ordinary optical fiber of length $L_j$. The purpose of this fiber is to provide delay equalization and its value will be determined in the analysis that follows. The light leaving the delay equalization fibers are summed and coupled to a

---

[24] R.A. Soref, "*Optical Dispersion Technique for Time-Delay Beam Steering,*" Applied Optics, Vol. 31, No. 35, pp. 7395-7397, 10 December 1992.

[25] M.Y. Frankel and R.D. Esman, *"True Time-Delay Fiber-Optic Control of an Ultrawideband Array Transmitter/Receiver with Multibeam Capability,"* IEEE Transactions on Microwave Theory and Techniques, Vol. 43,. No.9, pp. 2387-2394, September 1995.

[26] S.T. Johns, D.A. Norton, C.W. Keefer, R. Erdmann, and R.A. Soref, *"Variable Time Delay of Microwave Signals Using High Dispersion Fiber,"* Electronics Letters, Vol. 29, No. 6, pp. 555-556, 18 March 1993.

fixed length of HDOF of length $\ell$ which provides a wavelength-dependent time delay $\tau(\lambda_j)$ obtained from Equation (14).

This collection of optical signals, all of them now on a single optical fiber, are sent to the *signal routing element* (SRE), which acts as a wavelength demultiplexing system. The SRE, shown in Figure 11, uses broadband Bragg reflectors for demultiplexing[27]. It is seen in Figure 11 that the signal, *f(t)*, modulating wavelength $\lambda_j$ with delay $\tau(\lambda_j)$ would pass through any gratings for which the wavelength $\lambda_j$ fell outside the BRGs spectral passband $\Delta\lambda$ ($\lambda_j \notin \Delta\lambda$) and be reflected by the grating for which $\lambda_j \in \Delta\lambda$. The reflected signal is routed to the proper antenna element by an optical circulator or more efficiently with Mach-Zehnder based Bragg grating directional couplers which have an insertion loss of less than 0.5 dB with better than 99% coupling efficiency[28]. Even this loss limits the use of the present system for large arrays. For a large number of elements, an in-fiber Bragg grating tap can be used to replace the traditional broadband BRGs. These taps are fundamentally different from BRGs in that they couple light within a specific wavelength band into the fiber's cladding modes. This light can be extracted from the cladding with roughly 10-20 % efficiency. More importantly, the off-wavelength transmission is still nearly 100% as with any fiber grating structure[29].

---

[27] M.C. Farries, K. Sugden, D.C.J. Reid, I. Bennion, A. Molony, and M.J. Goodwin, "*Very Broad Reflection Bandwidth (44nm) Chirped Fiber Gratings and Narrow Bandpass Filters Produced by the use of an Amplitude Mask,*" Electronic Letters, Vol. 30, No. 11, pp. 891-892, 1994.

[28] F. Bilodeau, D.C. Johnson, S. Thériault, B. Malo, J. Albert and K.O. Hill, "*An all-fiber, dense wavelength division multiplexer / demultiplexer using photoimprinted Bragg gratings,*" IEEE Photonics Technology Letters, Vol 7, No 4, p. 388, 1995.

[29] G. Meltz, W.W. Morey, and W.H. Glenn, "*In-Fiber Bragg Grating Tap,*" in Technical Digest on Optical Fiber Communication, Optical Society of America, Washington, D.C., p.24, 1990.

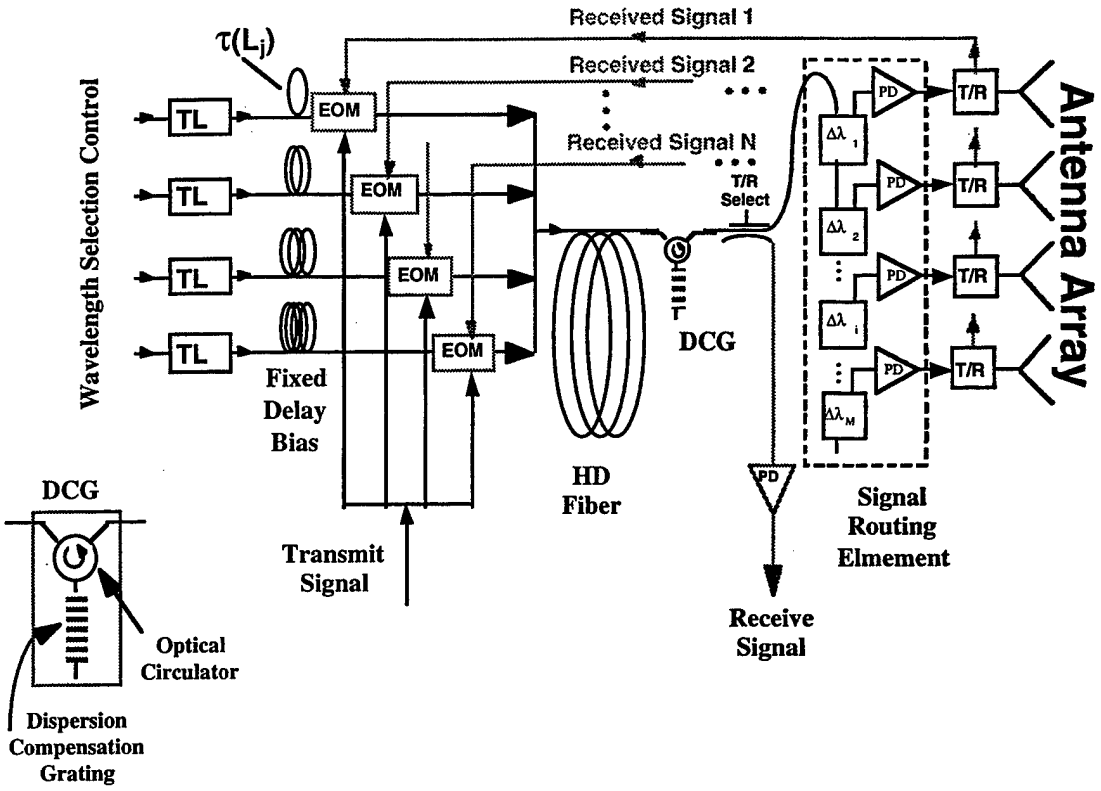


Figure 10. HDOF TTD transmit/receive architecture.

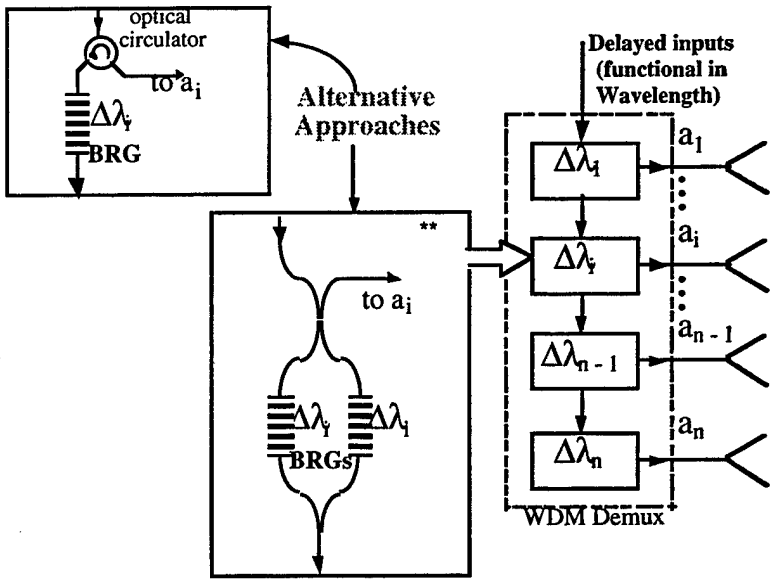


Figure 11. Signal routing element.

As mentioned earlier, the purpose of the delay equalization fiber is to compensate for path length differences between all the lasers and the detectors. The total time delay $T_j$ incurred by the microwave modulated optical signal emanating from laser j operating at wavelength $\lambda_j$ and arriving at array location j computed as

$$T_j = \tau(L_j) + \tau(\lambda_j) + 2\tau_j + \tau_{j-1} + \ldots + \tau_1. \quad (15)$$

As before $\tau(L_j)$ is the fixed fiber delay at the laser j output, $\tau(\lambda_j)$ is the wavelength dependent delay obtained from the dispersion fiber, and $\tau_j$ is the delay through the j-th wavelength routing element. The fiber lengths $L_j$ required to equalize delay are computed as follows: with all lasers operating at their respective center wavelengths, the time delay $T_j$ (and hence $L_j$) is chosen so that a particular radiation pattern, generally a broadside pattern results.

One problem associated with optical fiber-based systems of this type, especially those using long lengths of fiber, is the bandwidth limit imposed on the microwave signal by the fiber dispersion. The fiber dispersion of the optical carrier that is utilized to generate time delay, also broadens the microwave (modulation) signal, an undesired effect. Ordinary fiber has dispersion D ≈ 10 ps/km-nm @1550 nm, while high dispersion fiber has D ≈ 100 ps/km-nm ≈ 8 ps/GHz-km. This problem can be greatly reduced and theoretically eliminated by including a linearly chirped Bragg grating at the output of the high dispersion fiber as shown in Figure 10. Such a device compresses the dispersion broadened pulses by providing an inverse to the chirp imposed by the high dispersion fiber[30]. Broad optical bandwidths may necessitate the use of several chirped gratings connected in series. Each device would possess the same chirp rate but centered at staggered wavelengths that cover the required optical band. If N EOMs are used for the transmit mode then an alter-

[30] F. Ouellette, "*Dispersion Cancellation Using Linearly Chirped Bragg Grating Filters in Optical Waveguides*," Optics Letters, Vol. 12, No. 10, pp. 847-849, Oct. 1987.

native approach may be taken. This would be to "pre-distort" the output of each EOM with a chirped grating covering only the portion of the full spectral range tuned by that laser and compensate for the spreading that the signal will incur as it travels through the high dispersion fiber.

Array pattern synthesis techniques require that a continuous range of differential time delays $\Delta\tau_j$ be available to the array element. This range determines the spectral width $\Delta\lambda_j$ of the BRG passband, and is determined from Equation (14) as

$$\Delta\lambda_j = \frac{\Delta\tau_j}{D\,\ell} \tag{16}$$

The spectral passbands $\Delta\lambda_j$ for each array element are adjacent, with center wavelength $\lambda_i$. The tunable laser used to access array element *j* is operated at a center wavelength $\lambda_j$ and has a tuning range of $\Delta\lambda_j$. This tuning range and center wavelength must be chosen so that the differential time delay $\Delta\tau_i$ necessary to drive array element *i* be obtainable from the HD fiber.

For example, consider a linear antenna array of 20 elements with inter-element spacing of $\lambda_{RF}/2$. Assume a typical HDOF dispersion, D = 100psec/ km-nm. Additionally assume that the maximum steer angle desired is ± 60 degrees, which requires an inter-element delay of $(\lambda_{RF}/2c_o)sin(60^o)$. For a microwave signal wavelength $\lambda_{RF}$ = 5 cm (f = 6 GHz), the maximum inter-element delay (required by the last element) is about 832 ps. Equation (16) shows that a grating passband $\Delta\lambda$ = 5 nm requires the high dispersion fiber length to be 1.66 km.

Operation for receive is simpler than for transmit. Referring again to Figure 10, the received microwave signals modulate the outputs of the TLSs which are summed and

coupled into the HDOF where each received signal is appropriately time delayed. The optical T/R select switch directs the composite signal away from the SRE and into a spectrally broad photodetector. As seen in the figure the entire received signal delay is accomplished in a single element (the dispersion fiber) *after the signals are summed.* The ability to achieve efficient post summation signal delay is unique to the photonic processing approach shown here.

## 5.2 Application to Null Steering

The previous section described a photonic processor capable of continuously varying time delay to perform beamforming for a phased array antenna. The architecture facilitated reciprocal function (both transmit and receive) using common hardware. In addition to beamforming — even more importantly — this architecture can be modified slightly to enable broadband null steering to counter jammers or other interferers that threaten operation of the phased array. Null steering is the placement of a zero in the array factor aligned along a particular spatial coordinate. Such systems are used to minimize the signal degradation caused by multipath interference or to minimize the presence of an unwanted (and often dynamic) jamming signal(s). Applications of this architecture would include Global Positioning System (GPS) navigational systems and other low order (antenna arrays with a small number of elements) systems.

The directional characteristics of an N-element phased array may be expressed as a polynomial of degree (N - 1) (the array factor) and is given by[31]:

$$AF_N(\theta) = \prod_{n=1}^{N-1}(z - z_n) = \sum_{n=0}^{N-1} a_n z^n \qquad (17)$$

[31] D.E.N. Davies, "*Independent Angular Steering of Each Zero of the Directional Pattern for a Linear Array,*" IEEE Transactions on Antennas and Propagation, March 1967, pp. 296-298.

$z = \exp[jkd\sin(\theta)]$, $d$ is the antenna element spacing, $k = \omega/c$ is the free space wave number for radian frequency $\omega$, $c$ is the speed of light in free space, and $z_n = z(\theta_n)$ is a zero of the polynomial corresponding to a null at angular coordinate $\theta_n$. Note that a change in location of even one zero affects *all* the polynomial coefficients $a_n$. This means that in order to independently place the $(N-1)$ array factor zeros requires $(2^{N-1}-1)$ *independent* time delays. Additionally, the precise element-to-element amplitude and phase tracking over the entire band of interest must be maintained.

These suggest that the ability to steer independent *broadband* nulls is much more complicated than that of a corresponding *narrowband* phased array. This added complexity is seen in Equation (17). A term of the form $exp[j\, k_o d\, sin(\theta_1) + j\, k_o d\, sin(\theta_2)]$ requires a two delay line implementation to support broadband nulling. In the narrowband application, a phase shifter can be used to obtain a typical coefficient $a_n$ in the array factor polynomial, *but only at a single frequency.*

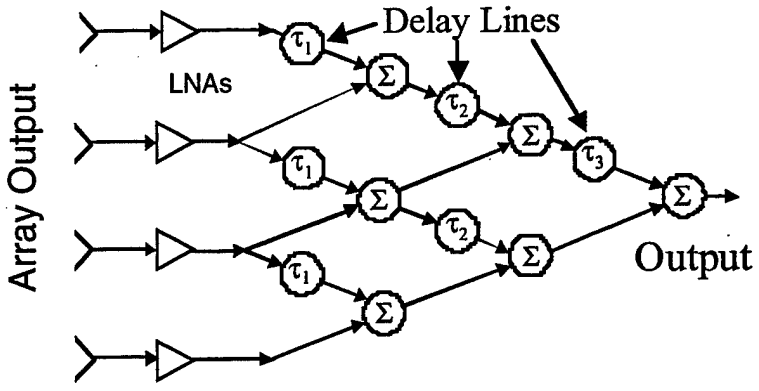


Figure 12. Schematic of arrangement for producing independent angular zero locations for a 4-element linear array.

Figure 12 shows a broadband realization of a nulling approach authored by Davies[32]. The output of each element is split into two, and the outputs combined in adjacent pairs via identical time delays $\tau_1$. The directional pattern of each element pair will be that of a two-element array and will produce one of the factors of Equation (17). We now apply the same procedure to the outputs of the three new groupings, now with time delay $\tau_2$, which produces the second factor in Equation (17). Clearly the overall pattern $AF_N(\theta)$ is obtained.

A broadband phased array null steering architecture achieving the requirements imposed by Equation (17) is shown in Figure 13. The architecture shown is very similar to that required for the receive function of the HDOF beamformer described above and shown in Figure 10. The differences are an increase in the number of TLSs from N-1 to $(2^{N-1} - 1)$ and the absence of BRGs for signal routing. Note, only the transmit function of the beamformer shown in Figure 10 required BRGs. Also note, in each architecture one laser can operate at a fixed wavelength and act as a reference. The system shown in Figure 13 performs null steering for a phased array antenna numbering 4 elements, the baseline configuration for GPS guided munitions. It requires 7 TLSs and a fixed reference laser and is capable of generating 3 independent broadband nulls.

Locating the 3 nulls along angular coordinates $\theta_1$, $\theta_2$, and $\theta_3$ , the array factor takes the form

$$\begin{aligned} AF_4(\theta) &= (e^{jkd\sin\theta} - e^{jkd\sin\theta_1})(e^{jkd\sin\theta} - e^{jkd\sin\theta_2})(e^{jkd\sin\theta} - e^{jkd\sin\theta_3}) \\ &= z^3 - z^2(e^{j\omega T_{21}} + e^{j\omega T_{22}} + e^{j\omega T_{23}}) + z(e^{j\omega T_{11}} + e^{j\omega T_{12}} + e^{j\omega T_{13}}) - e^{j\omega T_{01}} \\ &= a_3 z^3 + a_2 z^2 + a_1 z + a_0 \end{aligned} \tag{18}$$

[32] D.E.N. Davies, "*Independent Angular Steering of Each Zero of the Directional Pattern for a Linear Array,*" IEEE Transactions on Antennas and Propagation, March 1967, pp. 296-298.

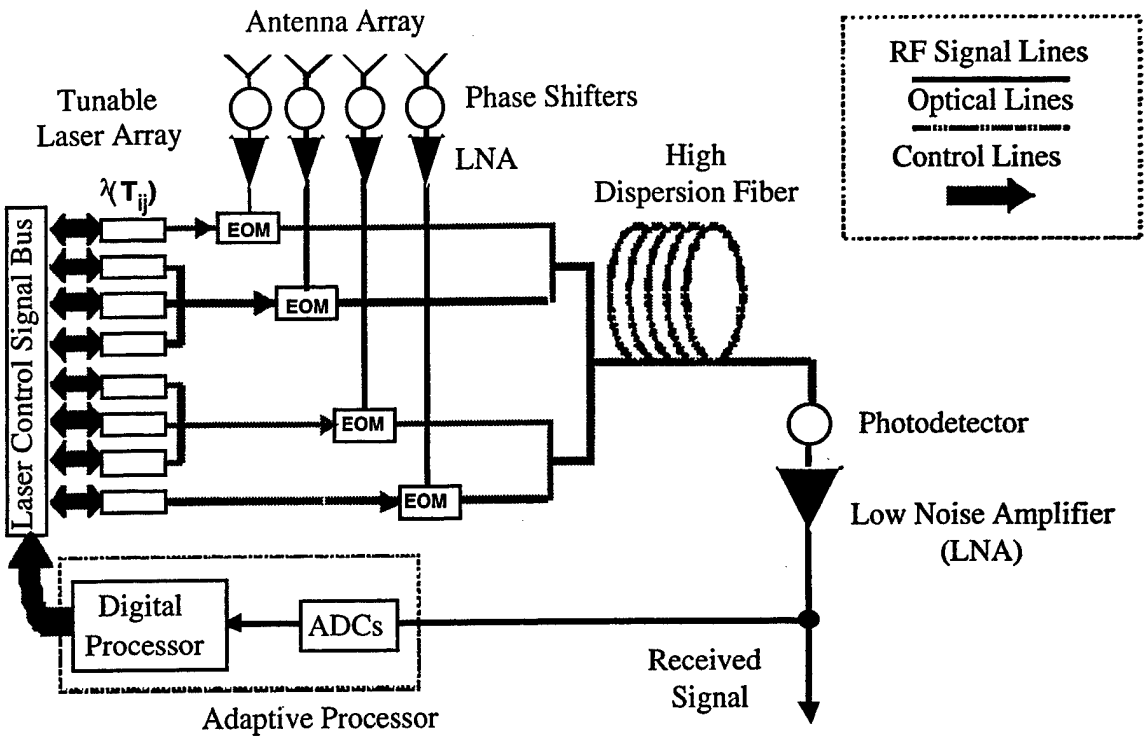


Figure 13. Photonic system for producing broadband nulls, shown for the case of a 4-element array capable of independently setting 3 zero locations.

The required differential time delays with $a_3$ as the reference element are:

$$T_{21} = \frac{d}{c}\sin\theta_1 \,, \; T_{22} = \frac{d}{c}\sin\theta_2 \,,$$

$$T_{23} = \frac{d}{c}\sin\theta_3 \,,$$

$$T_{11} = \frac{d}{c}(\sin\theta_1 + \sin\theta 2) \,,$$

$$T_{12} = \frac{d}{c}(\sin\theta_1 + \sin\theta_3) \,,$$

$$T_{13} = \frac{d}{c}(\sin\theta_2 + \sin\theta_3) \,,$$

$$T_{01} = \frac{d}{c}(\sin\theta_1 + \sin\theta_2 + \sin\theta_3) \,. \qquad (19)$$

These $N-1$ delays are obtained using the bank of tunable lasers shown in Figure 13. Each laser operates at a wavelength $\lambda(T_{ij})$ and has a tuning range $\Delta\lambda$ wide enough so that the necessary differential time delays specified above can be accessed via the HDOF. The laser outputs are optically summed in the groups shown using optical couplers so that when delayed they form the appropriate polynomial coefficients $a_0$, $a_1$, $a_2$, and so on. Negative coefficients are obtained by using a broadband electrical pi-phase shifter at the appropriate modulator inputs, and amplifiers can be included to equalize the electrical signal level. The amplified signal, from the antenna array element, modulates the optical carrier using an Electro-optic Modulator (EOM). Direct modulation of the lasers is possible so long as this modulation does not introduce a wavelength shift or an RF phase shift. The EOM outputs are summed and coupled in a single length of HDOF which provides the desired wavelength dependent delay on each set of optical carriers. The HDOF output is coupled to a spectrally broad photodetector (PD) which recovers the properly delayed and summed microwave antenna signals, which constitute the receiver output. For an adaptive system, a portion of this output as well as the outputs of each antenna elements would be digitized, and an appropriate algorithm would be used to adjust the laser operating wavelengths via the laser controller.

Regarding system loss, the optical power reaching the PD in Figure 13 is reduced by several factors. The major loss mechanisms are the couplers used to combine the laser outputs, with roughly 3-dB of loss for every two signals combined. The (N:1) summer used to combine the EOM outputs into the HDOF contributes a loss of $10 \log N$ dB plus excess loss, generally 1~2-dB. Generally, an EOM biased at quadrature contributes a total insertion loss of approximately 6 – 8 dB. The HDOF introduces a loss of 0.5 dB/km. Splices, connectors, isolators (if used) and the like will add another several dB of excess loss to the system. Since the system is fiber based, optical amplifiers can be incorporated into the design to compensate for the insertion losses of the system, however the effects

of added noise would have to be examined. Post detection electronics such as impedance matching, AGC circuitry, and the like would also be present in any phased array system and are not shown in the figure.

## 5.3 Experimental Set-Up

Figure 14 shows the experimental setup, constructed for the case of $N = 3$. We wanted to construct a 4 element (the baseline configuration for GPS guided munitions) demonstration system, but only had three modulators that were impedance matched at 1.2 GHz. This 3 element proof-of-concept breadboard is capable of 2 independent nulls.

Four thermally tunable diode lasers each with roughly a 2 nm tuning range were used as the optical sources. One laser always serves to provide a reference delay and need not be tunable. This reference laser and one other laser were coupled to individual EOM's while the outputs of the other two lasers were summed using optical coupler $c_1$ before being coupled into one EOM. Adjusting the laser drive currents equalized the optical output power of the EOM's. The shared EOM was driven by an electrical signal with a broadband 180° hybrid junction to provide the negative polynomial coefficient in the array factor. The remaining two EOM's were also driven by the 0° output of identical hybrid junctions to maintain similar impedance characteristics. The effect of the spatially distributed array elements can be simulated by splitting the output signal of the RF network analyzer and introducing excess electrical path lengths between the EOM electrical inputs. For the measured data presented in the following section, an equal path length split was used to simulate a broadside signal incident on the array. The optical outputs of the three EOM's were summed using the couplers $c_2$, $c_3$, and $c_4$ shown with the output of coupler $c_4$ fused to a 5-km length of HDOF manufactured by Lucent Technologies with a dispersion of $D = 101.6$ *psec/km-nm*. A broadband photodetector followed by a 20dB RF amplifier drove port-2 of the network analyzer. The laser operating wavelengths were

adjusted to provide nulls in the array factor at 0 and 60 degrees. Calibration of the measurement system described above was performed with respect to the reference laser and the necessary delay data was then measured using the network analyzer.

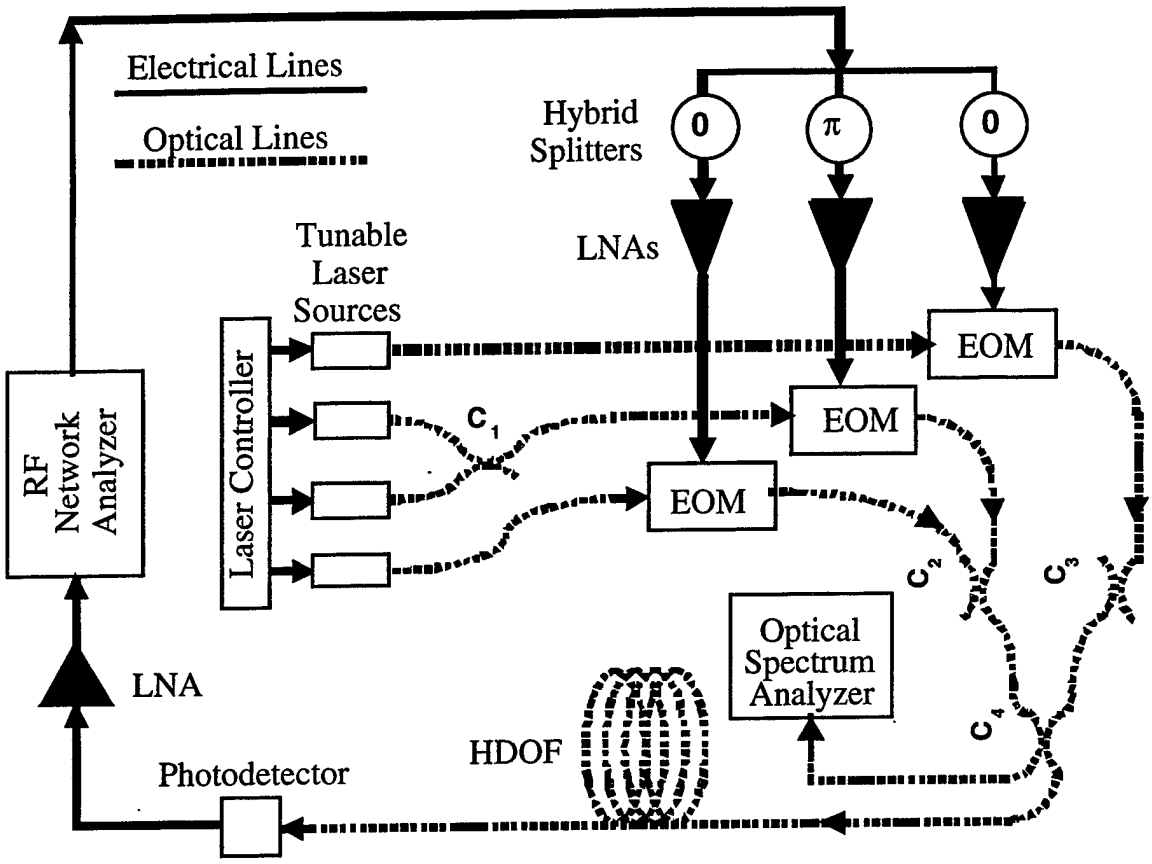


Figure 14. Experimental setup for a 3-element array proof-of-concept null steering breadboard.

Three nominally identical EOM modulators were used in the experimental setup shown in Figure 14, each capable of operating over a 7 GHz microwave bandwidth. Impedance measurements showed that modulators were not well matched over very broad bands (GHz). In fact the impedance matching characteristics limited operation to approximately 100 MHz bandwidth centered at 1.2 GHz, dictating the frequency range used in the measurements.

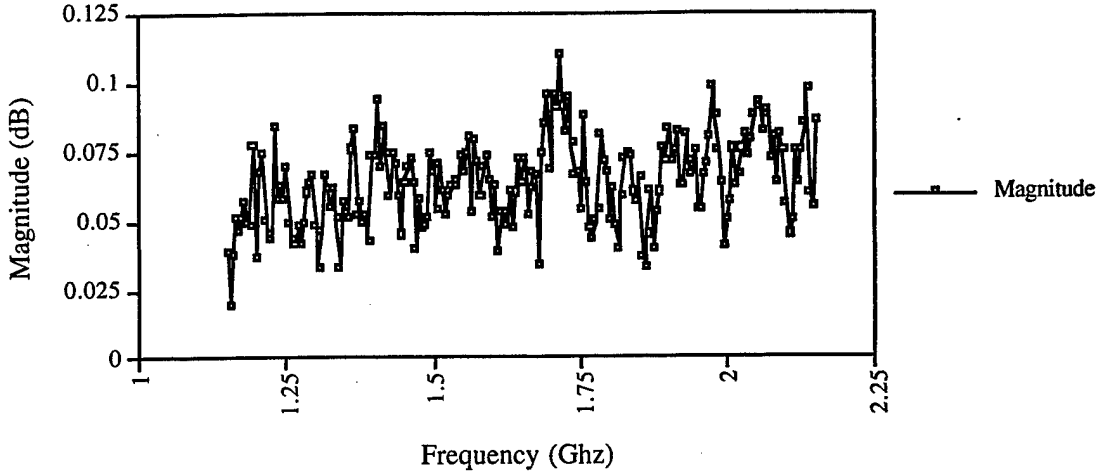


Figure 15. Typical magnitude data for the 3-element HDOF null steering system.

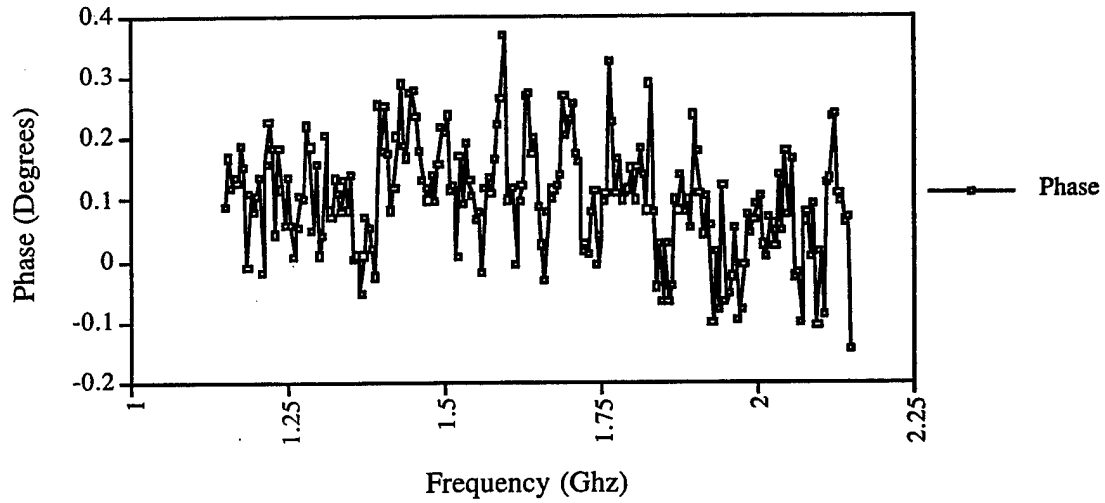


Figure 16. Typical phase data for the 3-element HDOF null steering system.

## 5.4 Discussion of Experimental Results

Figures 15 and 16 show typical measurements of magnitude and phase respectively for the HDOF null steering proof-of-concept breadboard. Phase and amplitude matching across the band govern the ability to obtain a given null depth over a specified bandwidth. The rms amplitude noise and phase noise across the entire band measured .05dB and 0.25° respectively. These measured values met the theoretical requirements (amplitude noise<0.1 dB and phase<0.25°) necessary to achieve a <-40 dB null depth. Figure 17 shows the null depth of the 3-element proof-of-concept breadboard versus frequency. The figure shows a uniform null depth of roughly -40dB across the full operating bandwidth. For comparison purposes, Figure 17 also shows the null that would result from an ideal phase shifter-based system. From this comparison, we see that the TTD processor provides an additional 20 dB of suppression at the band edges (1.15 GHz and 1.25 GHz). As applied to a 20 MHz bandwidth GPS receiver, the TTD processor provides an additional 15 dB of nulling at the band edges 1.19 GHz and 1.21 GHz.

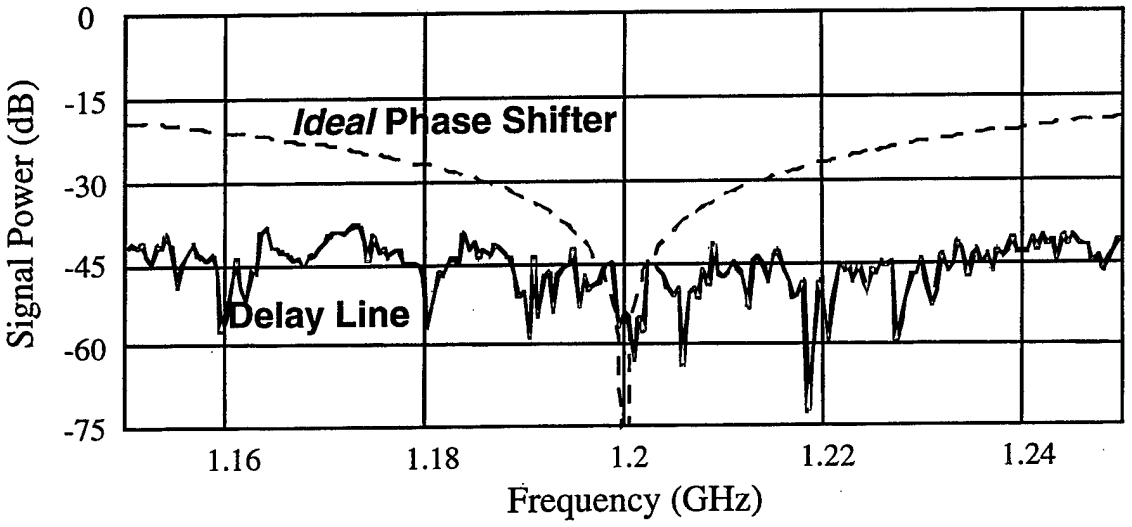


Figure 17. Null depth as a function of frequency for the 3-element HDOF system.

Impedance matching characteristics between channels limit the system's bandwidth. For the null steering demonstration system, off-the-shelf components were used. The electro-optic modulators turned out to be the limiting component for impedance matching. The null steering system displayed approximately 10% fractional bandwidth (100MHz). More closely matched modulators would yield a null steering system capable of several GHz of bandwidth. Beamforming rather than null steering applications have less stringent requirements for amplitude and phase matching. In fact, the demonstration system would be capable of several GHz of bandwidth for beamforming applications.

The HDOF introduces a lever arm effect, which enhances laser wavelength jitter effects proportional to the length of the fiber. As shown by Equation (14), the length of the HDOF depends on the maximum time delay, the dispersion, and the tuning range of the laser. The system requirements for GPS munitions guidance fix the maximum time delay and the dispersion is fixed @ 100ps/km-nm. The tuning range of the laser and the length of the HDOF are the variable parameters. Commercially available tunable lasers have tuning ranges in excess of 80nm and would have reduced the required HDOF length in the experimental setup by a factor of forty.

Reducing the length of the HDOF also will reduce the loss by 0.5 dB/km. This reduction in length will also minimize amplitude and phase noise critical to achieving null depth. Future plans include using lasers that tune over 50 nm allowing a reduction in length of the fiber from 5 km to <0.5 km.

# 6.0 Summary

This report has documented the impact of several relatively new photonic components coming to the forefront in applications related to the photonic processing of broadband microwave signals. Included in this set of photonic elements are the wavelength tunable laser, high dispersion optical fiber, and the Bragg reflection grating. Because of the efficiency and potential cost effectiveness offered by these components, they hold the promise of revolutionizing the field of broadband photonic processing. Practical commercial photonic processors are likely to become viable in the near term as a result of these new components. This report showed the performance characteristics of these components and how they can be used for two broadband phased array applications, beamforming and null steering. Two systems were described. Both systems maximize component reuse and allow fully integrated transmit and receive modes in one efficient hardware compressive topology.

The first TTD beamformer used a wavelength-tunable laser source, in conjunction with arrays of BRGs forming a fiber grating prism. This photonic architecture generated discrete time delays and could function in both tranmit and receive modes. A proof-of-concept transmit system was constructed. It demonstrated 3.5 GHz bandwidth high resolution *squint* free beamsteering with highly linear low-noise phase data (<2 degrees over the 3.5 GHz band). The receive function was not demonstrated due to the availability of only one EOM. A total of 4 EOMs were needed for a duplex (transmit/receive) system demonstration. No other additional hardware was required for duplex operation (see Figure 2). Although illustrated and demonstrated as fiber-based, this system could be integrated on a single substrate in the form of a photonic integrated circuit. Additionally, this architecture can be extended for use in antennas with large numbers (thousands) of

elements. In fact this very same approach is now being adopted by TRW for a satellite communications system design at EHF.

The second TTD processor used a wavelength-tunable laser source, in conjunction with a high dispersion optical fiber. This processor generates a continuum of time delays making it highly suitable for null steering, in addition to beamforming applications. An architecture for beamforming (both transmit and receive) was developed. The receive portion of this architecture was modified slightly to facilitate broadband null steering. The modification increased the number of tunable lasers from N-1 to $(2^{N-1} - 1)$. Where N is the number of antenna elements in the phased array. This requirement of having $(2^{N-1} - 1)$ tunable lasers limits application of the null steering processor to small order arrays ($N \sim 6$) due to complexity and cost. The null steering processor developed has wide applicability in telecommunications and navigation applications where small platforms constrain the array size to only a few elements.

Our target application is null steering for GPS guided munitions, which have a 4 element phased array. We constructed a proof-of-concept null steering processor that demonstrated -40dB null depth across 100 MHz bandwidth centered at 1.2 GHz. This translates to an additional 20 dB of suppression as compared with a phase shift system at the band edges 1.15 GHz and 1.25 GHz. As applied to a 20 MHz bandwidth GPS receiver, the system provides a 15dB improvement at the band edges 1.19 GHz and 1.21 GHz.

We plan to continue development of the null steering processor to fulfill requirements for GPS guided munitions in cooperation with the AFRL Munitions Directorate. This work will be the subject of a future report.